Virginia Tech Comprehensive Power-based Fuel Consumption Model (VT-CPFM): Model Validation and Calibration Considerations

Sangjun Park[a], Hesham A. Rakha[b,*], Kyoungho Ahn[c] and Kevin Moran[d]

[a]Department of Civil Engineering, Chosun University, 309 Pilmun-daero Dong-gu Gwangju 501-759, South Korea,Phone: 82-62-230-7089, Fax: 82-62-220-2687 spark.vt@gmail.com

[b]Charles E. Via, Jr. Department of Civil and Environmental Engineering, 3500 Transportation Research Plaza, Blacksburg, VA 24061 Phone: (540) 231-1505; Fax: (540) 231-1555

[c]Center for Sustainable Mobility, Virginia Tech Transportation Institute, 3500 Transportation Research Plaza, Blacksburg, VA 24061 Phone: (703) 538-8447; Fax: (540) 231-1555 kahn@vt.edu

[d]Nokia Here, 425 West Randolph Street, Chicago, IL 60606 Phone: (312) 894-7601; Fax: (312) 894-8441 kevin.moran@nokia.com

ABSTRACT

A power-based vehicle fuel consumption model, entitled the Virginia Tech Comprehensive Power-based Fuel Consumption Model (VT-CPFM) that was developed in an earlier publication is validated against in-field fuel consumption measurements. The study demonstrates that the VT-CPFMs calibrated using the EPA city and highway fuel economy ratings generally provide reliable fuel consumption estimates with a coefficient of determination in the range of 0.96. More importantly, both estimates and measurements produce very similar behavioral changes depending on engine load conditions. The VT-CPFMs are demonstrated to be easily calibrated using publically available data without the need to gather in-field instantaneous data.

1. INTRODUCTION

A new power-based microscopic fuel consumption model entitled the Virginia Tech Comprehensive Power-based Fuel Consumption Model (VT-CPFM) was developed in order to provide reliable fuel consumption estimates and convenience of easy calibration

*Corresponding Author Email addresses: hrakha@vt.edu

[1]. Specifically, the VT-CPFM can be easily implemented in systems that require use of a microscopic-level fuel consumption model including microscopic simulation software and eco-cruise control systems. The newly developed model meets the requirements for the predictive eco-cruise control system in the sense that it overcomes two major drawbacks of existing fuel consumption models. First, the VT-CPFM model does not produce a bang-bang control system while the existing fuel consumption models do. Second, the VT-CPFM model is easily calibrated using the Environmental Protection Agency (EPA) city and highway fuel economy ratings and publicly available vehicle and roadway pavement parameters, thus it does not require in-laboratory or field data collection that is typically required to calibrate existing fuel consumption models [1].

The VT-CPFM was validated regarding instantaneous fuel consumption measurements, trip fuel consumption estimates, and optimum cruise speeds. For the validation of instantaneous fuel consumption measurements, one light-duty truck (Ford Explorer) and two light-duty passenger cars (Saturn SL and Honda Accord) were tested on three drive cycles on a chassis dynamometer: 1) the arterial level of service (LOS) A cycle, 2) the LA92 cycle, and 3) the New York cycle [1]. The plots of the measured and estimated fuel consumption rates demonstrated an good agreement. The VT-CPFM seemed to overestimate some fuel consumption rates for the New York cycle, but the model estimation generally provided high coefficients of determination (94% to 98%) compared to the measured fuel consumption rates. For the validation of trip fuel consumption estimates, the aggregated total fuel consumed by the three vehicles on 16 drive cycles that represented different roadway types and different levels of congestion was compared to the VT-CPFM estimates. The comparison showed an ideal fit between the model estimates and the field measurements. Finally, the VT-CPFM was found to be consistent with the VT-Micro predictions of optimum cruise speeds and produced the same bowl-shaped curve as a function of vehicle cruise speed.

The VT-CPFM provides reliable estimates compared to the field-measured fuel consumption rates. However, the aforementioned validation efforts mostly relied on chassis dynamometer tests and predefined drive cycles. Given that the objective of the VT-CPFM development is to use the model as a critical component for eco-friendly systems such as predictive eco-cruise control systems (ECCs), it would be beneficial to assess its performance on actual roadways under real-world driving conditions. Furthermore, the performance evaluation is meaningful in the sense that fuel consumption rates under manual and conventional cruise control driving conditions may be of interest. Therefore, the objective of this study is to quantify the performance of the VT-CPFM considering various vehicles on real roadway sections under either manual or conventional cruise control driving conditions.

In terms of paper layout, the overview of the VT-CPFM is provided in the first section. The field test efforts are then described, focusing on the experimental design and the calibration of the VT-CPFM parameters for the test vehicles. Next, given the calibrated models, the VT-CPFM is validated with regard to the estimation of instantaneous fuel consumption rates and fuel economy values. Finally, the summary findings and conclusions are presented.

2. OVERVIEW OF THE VT-CPFM

A second-order polynomial model was used as the framework of the VT-CPFM because the relationship between fuel consumption rates and positive power conditions collected by an Onboard Diagnostic (OBD) reader were demonstrated to be convex as shown in Figure 1. Consequently, two simple power-based fuel consumption models were proposed as second-order polynomial models as formulated in Equations (1) and (2). The framework provides two merits: 1) It does not result in a bang-bang control and 2) The model can be calibrated using the EPA city and highway cycles [1].

$$FC(t) = \begin{matrix} \alpha_0 + \alpha_1 P(t) + \alpha_2 P(t)^2 & \forall\, P(t) \geq 0 \\ \alpha_0 & \forall\, P(t) < 0 \end{matrix}, \quad \text{and} \tag{1}$$

$$FC(t) = \begin{matrix} \beta_0 \omega_e(t) + \beta_1 P(t) + \beta_2 P(t)^2 & \forall\, P(t) \geq 0 \\ \beta_0 \omega_{idle} & \forall\, P(t) < 0 \end{matrix}. \tag{2}$$

Where α_0, α_1, α_2 and β_0, β_1, and β_2 are vehicle-specific model constants that are calibrated for each vehicle, and ω_{idle} is the engine idling speed (rpm). In the case of the VT-CPFM-1 model the power exerted at any instant *t* is computed using Equation (3).

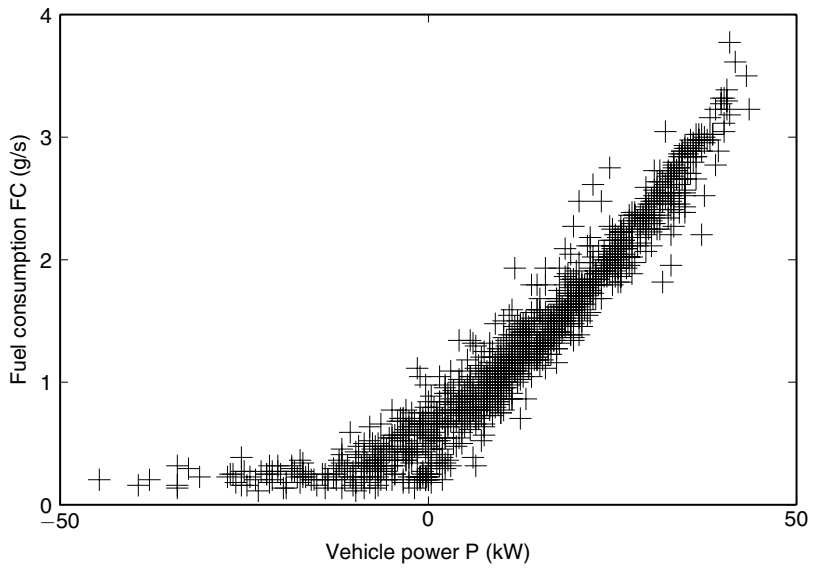

Figure 1. Typical power versus fuel consumption functional form

$$P(t) = \left(\frac{R(t) + 1.04ma(t)}{3600\eta_d} \right) v(t). \tag{3}$$

As can be seen in Equations (1) and (2), the VT-CPFM-1 model does not require any engine data while the VT-CPFM-2 model does require engine data. Consequently, the VT-CPFM-1 model is suitable for implementation within microscopic traffic simulation software, and the VT-CPFM-2 model can be used to develop predictive, eco-gear-shifting strategies as the engine speed term can capture the effects of gear shifting.

The idling fuel consumption rate for the VT-CPFM-1 model is calibrated using Equation (4). The use of the max function ensures that the functional form is convex.

$$\alpha_0 = \max \left(\frac{P_{mfo}\omega_{idle}d}{22164 \times QN}, \frac{\left(F_{city} - F_{hwy}\frac{P_{city}}{P_{city}} \right) - \varepsilon \left(P^2_{city} - P^2_{hwy}\frac{P_{city}}{P_{hwy}} \right)}{T_{city} - T_{hwy}\frac{P_{city}}{P_{city}}} \right) \tag{4}$$

Here P_{mfo} is the idling fuel mean pressure (400,000 Pa); ω_{idle} is the idling engine speed (rpm); d is the engine displacement (liters); Q is the fuel lower heating value (43,000,000 J/kg for gasoline fuel); N is the number of engine cylinders; F_{city} and F_{hwy} are the total fuel consumed for the EPA city and highway drive cycles (liters), respectively (computed using Equations (5) and (6), respectively); T_{city} and T_{hwy} are the durations of the city and highway cycles (1875s and 766s, respectively); and P_{city} and P^2_{city} are computed as the sum of power and power squared exerted each second over the entire cycle (computed using Equations (7) and (8), respectively). Similarly, P_{hwy} and P^2_{hwy} are estimated in the same manner for the highway cycle. The ε term ensures that the second-order parameter (α_2) is greater than zero. Experimentation with the model revealed that a minimum value of 1E-06 ensures that the optimum fuel economy cruising speed is in the 60 to 80 km/h range which is typical of light-duty vehicles.

$$F_{city} = \frac{3.7854 \times 17.663}{1.6093 \times FE_{city}} = \frac{41.5546}{FE_{city}} \tag{5}$$

$$F_{hwy} = \frac{3.7854 \times 16.4107}{1.6093 \times FE_{hwy}} = \frac{38.6013}{FE_{hwy}} \tag{6}$$

$$P_{city} = \sum_{t=0}^{T_{city}} P(t) \text{ and } P_{hwy} = \sum_{t=0}^{T_{hwy}} P(t) \tag{7}$$

$$P_{city}^2 = \sum_{t=0}^{T_{city}} P(t)^2 \text{ and } P_{hwy}^2 = \sum_{t=0}^{T_{hwy}} P(t)^2 \tag{8}$$

It should be noted that the EPA started the use of additional drive cycles in 2008. These new tests—they had, in fact, been in use since the late 1990s but for emissions purposes only—are the US06 high-speed (80 mph max) cycle; the SC03, or "A/C," cycle, which is very similar to the city cycle but runs in 95-degree heat with the vehicle's air conditioning active; and the cold FTP test, which is exactly the same as the city cycle but runs at a temperature of 20 °C. Until the 2012 model year, automakers ran the tests on the old drive cycles but reported the fuel-economy ratings for the new cycles using Equations (9) and (10) developed by the EPA. Here FE_{city} and FE_{hwy} are the fuel economy estimates for the old cycles while FE'_{city} and FE'_{hwy} are the estimates for the new drive cycles. It should be noted that the units of FE are in mi/gal in the case of U.S. cycles.

$$FE'_{city} = \frac{1}{\frac{1.18053}{FE_{city}} + 0.003259} \tag{9}$$

$$FE'_{hwy} = \frac{1}{\frac{1.3466}{FE_{hwy}} + 0.001376} \tag{10}$$

In order to ensure that the fuel consumption versus vehicle power relationship is convex, a constraint is introduced. Specifically, this constraint ensures that α_2 is positive and the α_1 can then be computed, as demonstrated in Equations (11) and (12). The parameter α_2 has to be greater than zero in order to ensure that the model does not produce a bang-bang control system [2].

$$\alpha_1 = \frac{F_{hwy} - T_{hwy}\alpha_0 - P_{hwy}^2\alpha_2}{P_{hwy}} \tag{11}$$

$$\alpha_2 = \frac{\left(F_{city} - F_{hwy}\frac{P_{city}}{P_{hwy}}\right) - \left(T_{city} - T_{hwy}\frac{P_{city}}{P_{hwy}}\right)\alpha_0}{P_{city}^2 - P_{hwy}^2\frac{P_{city}}{P_{hwy}}} \geq \varepsilon = 10\text{E-}06 \tag{12}$$

Once α_0 is computed, the remaining two model coefficients (α_1, α_2) can be estimated using the fuel economy ratings for the EPA city and highway drive cycles. As shown in Equation (13), the two variables α_1 and α_2 can be computed by solving a system of two linear equations as

$$\begin{aligned} F_{city} &= T_{city}\alpha_0 + P_{city}\alpha_1 + P_{city}^2\alpha_2 \\ F_{hwy} &= T_{hwy}\alpha_0 + P_{hwy}\alpha_1 + P_{hwy}^2\alpha_2 \end{aligned}. \tag{13}$$

The VT-CPFM-2 model that was presented earlier in Equation (2) can be calibrated in a similar fashion. The engine speed coefficient is computed as

$$\beta_0 = \frac{P_{mfo}d}{22164 \times QN}. \tag{14}$$

The two remaining parameters can then be calibrated using the EPA fuel economy ratings for the city and highway cycles using Equations (15) and (16).

$$\beta_1 = \frac{\left(\frac{F_{city} - \omega_{city}\beta_0 - P_{city}^2\beta_2}{P_{city}}\right) + \left(\frac{F_{hwy} - \omega_{hwy}\beta_0 - P_{hwy}^2\beta_2}{P_{hwy}}\right)}{2} \tag{15}$$

$$\beta_2 = \frac{\left(F_{city} - F_{hwy}\frac{P_{city}}{P_{hwy}}\right) - \left(\omega_{city} - \omega_{hwy}\frac{P_{city}}{P_{hwy}}\right)\beta_0}{P_{city}^2 - P_{hwy}^2\frac{P_{city}}{P_{hwy}}} \geq 1\text{E-}06 \tag{16}$$

All terms are similar to the earlier definitions except for the ω_{city} and ω_{hwy} parameters that are computed using Equations (17) and (18).

$$\omega_{city} = \sum_{t=0}^{T_{city}} \omega(t) \tag{17}$$

$$\omega_{hwy} = \sum_{t=0}^{T_{hwy}} \omega(t) \tag{18}$$

3. EXPERIMENTAL DESIGN AND VT-CPFM CALIBRATION

3.1. Collection of Field Data

Experiments were conducted on a section of Interstate 81 between mile markers 118 and 132 in order to collect fuel consumption rates under actual driving conditions. The test section was selected because it comprises various uphill and downhill sections and thus provides a suitable environment to test different engine load conditions under manual and CCC driving scenarios. Specifically, the northbound and the southbound directions entail an overall 1.3% downhill and a 1.3% uphill section, respectively, as the difference in altitude between the start and end points of the section is approximately 280 m across 22.4 km (14 miles). However, the roadway grade on the section varies between $\pm$ 4%. There are two 4% uphill sections that have an additional truck-climbing lane in the southbound direction.

Six light-duty vehicles were tested, including four passenger cars and two sport utility vehicles (SUVs). These vehicles included: a 2001 SAAB 95, a 2006 Mercedes R350, a 2008 Chevy Tahoe, a 2007 Chevy Malibu, a 2008 Hybrid Chevy Malibu, and a 2011 Toyota Camry. The six vehicles were selected to test different manufacturers, model years, and vehicle types. The Chevy Tahoe was the heaviest and most powerful vehicle while the Malibu was the lightest and least powerful vehicle. The SAAB 95 was the oldest vehicle and had a turbocharged engine generating relatively more power than the other passenger cars when considering their engine sizes.

For the data collection an OBD II reader (the DashDaq XL device that is manufactured by Drew Technologies, Inc.) was used. The DashDaq can be easily attached to a window using a shield mount and can log and save up to 16 user-defined parameters [3]. This study selected the following 16 signals to record: absolute throttle position, fuel economy across distance, engine speed, vehicle speed, acceleration level, vehicle power, GPS-calculated speed, latitude, longitude, torque, calculated mass air flow, altitude, air flow rate from mass air flow, accelerator pedal position, fuel economy over time, and fuel level. The signals were saved to a Secure Digital (SD) card with a timestamp. The vehicle signals continued to be displayed on the screen as they were being saved to the card.

Given that the DashDaq provides the fuel economy in units of miles per gallon (MPG) along with a timestamp, instantaneous fuel consumption rates can be calculated from the recorded data. Specifically, the DashDaq calculates the fuel economy using the vehicle speed and mass air flow signals together with two assumptions. The first assumption is that the stoichiometric ratio, also called air-fuel ratio, is 14.7. The density of fuel is assumed to be 720 grams per liter. The fuel economy can then be calculated using Equation (19). Note that the first assumption is not 100% accurate given that the air-fuel ratio does not remain constant and can vary depending on the required power levels. In other words, it does not capture fuel-rich and fuel-lean conditions accurately, so the fuel estimation from this approach may slightly deviate from the true value.

$$FE = \frac{vsd}{a} \tag{19}$$

Where FE is the fuel efficiency in mi/gal, v is the velocity of the vehicle in miles per hour (mph), s is the stoichiometric ratio, d is the density of fuel in grams per gallon, and a is the mass air flow in grams per hour.

The experiments were conducted during off-peak hours between 9 a.m. and 3 p.m. in order to reduce conflicts with other vehicles and secure freedom of driving. Each vehicle was driven 10 times (circulations between mile markers 118 and 132) by two different drivers: five times with the CCC enabled and five times with the CCC disabled. Consequently, four data sets were obtained for each vehicle: the northbound with and without CCC enabled and the southbound with and without CCC enabled. There was an exception with the Toyota Camry due to a roadway maintenance event. Only six circulations were completed, and the last of the experiments could not be conducted due to the limited use of the roadway. The drivers participating in the study were educated about the overall procedures before the experiments. Specifically, the drivers were directed to maintain the highway speed limit of 65 mph in a typical driving manner while the CCC was not used (manual). However, some deviations from the target speed were allowed as needed in order to secure the driver's safety. For the CCC driving experiments, the target speed was also set to 65 mph. The drivers were allowed to turn off the CCC system for their safety as needed.

The specifications of the test vehicles were gathered using publicly available data sources, which included the vehicle manuals, the official sites of the vehicle manufacturers, and other car review sites [4]. Additionally, information about the vehicles was retrieved using the vehicle identification numbers (VINs) [5]. The specification information collected from different data sources was verified before calibrating the coefficients of the Virginia Tech Comprehensive Power-based Fuel Model (VT-CPFM). For cases in which the specifications could not be obtained from the aforementioned sources, typical values were used during the calibration [6]. These included the coefficients of roadway friction and the coefficients of rolling resistance.

The specifications that were used to calibrate the VT-CPFM models are shown in Table 1 along with the data sources. The VT-CPFM parameters were calibrated using a calibration tool that was developed in the MATLAB environment and described in detail in the literature [1].

4. VALIDATION OF THE VT-CPFM

4.1. Instantaneous Fuel Consumption Rates

Given the calibrated VT-CPFM parameters, the fuel consumption estimates and measurements were compared to validate the performance of the VT-CPFM and the calibration procedure. In order to calculate the instantaneous fuel consumption rates, the power levels were first computed given that they are required as inputs to the model. Roadway grade, which is used to compute the grade-resistance force, was initially calculated using the x, y coordinates and height signals collected by the GPS unit. However, the resolution of the GPS height signal was found to not be sufficiently accurate for computational purposes. Thus, higher resolution geographical data were obtained from NAVTEQ and were used to compute the grade-resistance force.

Given the field-measured fuel consumption rates and model estimates, the quality of the fuel estimates were first assessed using scatter plots. Specifically, the field-measured

Table 1. Specifications of the test vehicles

Description	Saab 95	Mercedes R350	Tahoe	Malibu	Malibu Hybrid	Camry	Source
Trim	4dr Sedan base	Base	LS 2WD	LS	Base	LE	
Model Year	2001	2006	2008	2007	2008	2011	
Wheel Radius	0.32145	0.36865	0.4014	0.32375	0.3322	0.3322	
Redline RPM	6000	6400	7000	6000	6000	6300	
Drag Coefficient	0.29	0.31	0.39	0.34	0.34	0.28	
Frontal Area (m2)	2.288	2.911	3.456	2.318	2.313	2.424	
Wheel Slippage	0.035	0.035	0.035	0.035	0.035	0.035	
Number of Cylinders	4	6	8	4	4	4	
Engine Size (L)	2.3	3.5	5.3	2.2	2.4	2.5	
Number of Gears	4	7	4	4	4	6	
First-gear Ratio	3.67	4.38	3.06	2.96	2.96	3.54	Auto
Second-gear Ratio	2.1	2.86	1.63	1.62	1.62	2.05	website
Third-gear Ratio	1.39	1.92	1	1	1	1.38	
Fourth-gear Ratio	1	1.37	0.7	0.68	0.68	0.98	
Fifth-gear Ratio	–	1	–	–	–	0.74	
Sixth-gear Ratio	–	0.82	–	–	–	0.66	
Seventh-gear Ratio	–	0.73	–	–	–	–	
Final Drive Ratio	2.56	3.9	3.23	3.63	3.63	3.82	
Mass (kg)	1601	2190	2388	1440	1604	1500	
City Fuel Efficiency (mpg)	21	16	14	24	24	22	
Hwy Fuel Efficiency (mpg)	30	21	20	34	32	33	
Rolling Coefficient(C_r)	1.75	1.75	1.75	1.75	1.75	1.75	Rakha *et al.*, 2001
c_1	0.0328	0.0328	0.0328	0.0328	0.0328	0.0328	
c_2	4.575	4.575	4.575	4.575	4.575	4.575	
Driveline Efficiency	0.92	0.92	0.92	0.92	0.92	0.92	
P_{mfo} (Pa)	400000	400000	400000	400000	400000	400000	Wong, 2001
Q (J/kg)	43000000	43000000	43000000	43000000	43000000	43000000	
Idling Speed (rpm)	820	700	600	680	660	660	Field Data

fuel consumption rates were plotted along the x-axis, and the model estimates were plotted along the y-axis. A regression line was then fitted to the scattered data points so that one can visually determine the level of match to the field observations, as illustrated

in Figure 2. Note that the regression line was forced to intersect with the origin (0, 0) when fitting to the data. The slope of the line indicates whether the VT-CPFM overestimates or underestimates the field measurements. The coefficient of determination indicates the degree of error that the model produces. For example, the slope of the regression line in Figure 2: is 0.93 demonstrating that the model underestimates the fuel consumption levels by 7 percent (on average). The R^2 value of the regression line is 0.9817, which is very close to 1. This implies that the model has a marginal error of less than 2 percent.

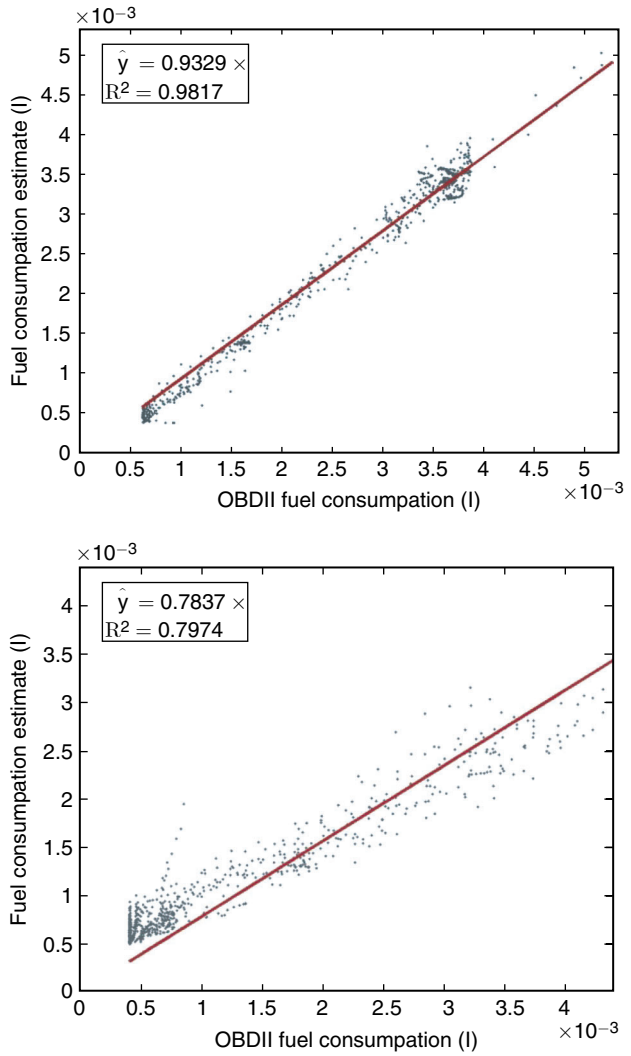

Figure 2. Fuel measurements versus fuel estimates scatter plots with a regression line

The instantaneous estimated and measured fuel consumption levels for each of the trips (i.e., the speed profiles along the study section) are compared and summarized in Table 2. The slope and R^2 values were averaged by vehicle type (six vehicles), driving direction (southbound and northbound), and driving type (manual and CCC driving). The results demonstrate that the performance of the VT-CPFM mainly depend on the vehicle type regardless of the driving direction and driving type. It is demonstrated that the fuel consumption rates estimated by the VT-CPFM-1 models were generally greater than those estimated by the VT-CPFM-2 models.

The VT-CPFM model estimates for the SAAB 95 and the Mercedes R350 appeared to be overestimated. However, their R^2 values were still very close to 1, demonstrating that the models provided ideal estimates that follow the same trends as observed from the OBD reading estimates.

Table 2. Average slope and R^2 values for the regression lines

			VT-CPFM-1		VT-CPFM-2	
Classification			Slope	R^2	Slope	R^2
Saab 95	Southbound	Manual	1.40	0.95	1.18	0.96
		Cruise	1.43	0.96	1.19	0.97
	Northbound	Manual	1.37	0.95	1.19	0.97
		Cruise	1.42	0.96	1.22	0.98
Mercedes R350	Southbound	Manual	1.61	0.95	1.46	0.96
		Cruise	1.62	0.96	1.46	0.96
	Northbound	Manual	1.56	0.93	1.42	0.95
		Cruise	1.62	0.96	1.48	0.97
Chevy Tahoe	Southbound	Manual	1.04	0.95	0.92	0.95
		Cruise	1.02	0.94	0.90	0.94
	Northbound	Manual	1.11	0.95	0.99	0.95
		Cruise	1.13	0.94	1.00	0.93
Chevy Malibu	Southbound	Manual	1.26	0.95	1.01	0.95
		Cruise	1.32	0.97	1.04	0.97
	Northbound	Manual	1.29	0.96	1.04	0.98
		Cruise	1.29	0.97	1.04	0.97
Hybrid Chevy Malibu	Southbound	Manual	0.97	0.94	0.82	0.95
		Cruise	0.93	0.98	0.79	0.97
	Northbound	Manual	0.97	0.96	0.85	0.98
		Cruise	0.94	0.97	0.82	0.98
Toyota Camry	Southbound	Manual	0.94	0.92	0.72	0.91
		Cruise	0.96	0.90	0.74	0.90
	Northbound	Manual	0.98	0.90	0.76	0.83
		Cruise	1.02	0.87	0.79	0.80

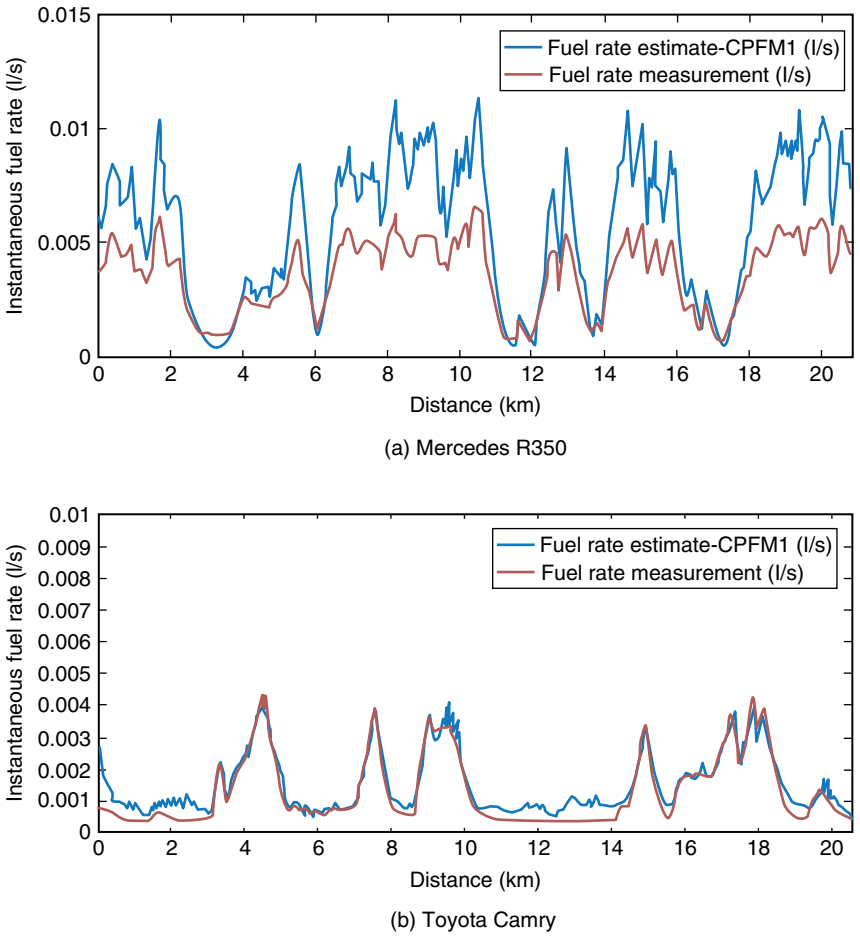

Figure 3. Fuel consumption profile on a test run

Figure 3 shows that the fuel estimates follow the same peaks and valleys observed during the field measurements, although the fuel consumption rates estimated by the Mercedes R350 model are higher than the fuel measurements. Overall, the VT-CPFMs were shown to provide ideal estimates given that the R^2 values were very close to 1. All R^2 values were greater than 0.85. Specifically, the profile shown in Figure 3(b) is one that has the lowest R^2 values, but still shows a good match to the field measurements.

4.2. Comparison of Fuel Economy Ratings

The fuel economy values estimated using the VT-CPFM models were compared to the field-measured values to determine the level of consistency at the aggregate trip level. The average fuel economy values and relative differences are summarized in Table 3. Given that some of the models overestimated the fuel consumption levels, the estimated fuel economy rates were lower than the field measurements. Specifically, the

Table 3. Fuel economy and relative difference

Classification			Fuel efficiency (km/L)			Relative difference	
			OBD-II	CPFM-1	CPFM-2	CPFM-1	CPFM-2
Saab 95	SB	Manual	10.9	8.0	9.3	−27%	−14%
		Cruise	11.4	8.1	9.6	−29%	−16%
	NB	Manual	17.9	14.0	15.1	−22%	−16%
		Cruise	19.9	15.2	16.2	−24%	−19%
Mercedes R350	SB	Manual	8.2	5.2	5.8	−36%	−30%
		Cruise	8.4	5.3	5.9	−36%	−30%
	NB	Manual	14.0	10.0	10.6	−29%	−24%
		Cruise	15.3	10.3	11.0	−33%	−28%
Chevy Tahoe	SB	Manual	7.5	7.2	8.1	−3%	9%
		Cruise	7.4	7.3	8.3	−1%	11%
	NB	Manual	14.0	11.9	13.4	−15%	−4%
		Cruise	14.6	12.1	13.5	−17%	−7%
Chevy Malibu	SB	Manual	11.8	9.4	11.7	−20%	0%
		Cruise	12.3	9.5	11.9	−23%	−4%
	NB	Manual	19.9	16.2	19.1	−19%	−4%
		Cruise	20.0	16.0	19.0	−20%	−5%
Hybrid Chevy Malibu	SB	Manual	11.0	11.6	13.5	5%	22%
		Cruise	10.9	11.9	13.7	9%	26%
	NB	Manual	17.8	19.2	20.8	8%	17%
		Cruise	18.9	21.1	22.4	11%	18%
Toyota Camry	SB	Manual	11.9	12.4	16.2	5%	36%
		Cruise	12.0	12.2	15.8	2%	31%
	NB	Manual	21.1	19.9	24.7	−6%	17%
		Cruise	21.5	19.3	24.1	−10%	12%

differences in fuel efficiency estimates between the VT-CPFM-1 model and OBD estimates ranged from −36 to +11 percent, while those of the VT-CPFM-2 model ranged from −30 to +36 percent. Consequently, it appears that the VT-CPFM-2 model produced greater differences as compared to the field measurements.

Given that the fuel consumption models are used for comparison of alternative scenarios, the fuel economy estimates are compared in terms of relative differences. In other words, it is important to evaluate the effectiveness of the models in identifying the optimum scenario. For this analysis, the manual and CCC driving scenarios were compared with regard to fuel economy. Additionally, driving on Interstate 81 northbound and southbound were compared. The fuel economy values that were averaged across all vehicles by the driving direction and the driving mode are summarized in Table 4. The field data indicate that the fuel economy was 4.1 percent greater when the CCC system was engaged, demonstrating that the CCC driving is better than manual driving in terms of fuel economy. The VT-CPFM-1 and -2 model

Table 4. Fuel economy averaged across all vehicles

Classification		Fuel efficiency (km/L)		
		OBD-II	CPFM-1	CPFM-2
SB	Manual	10.21	8.98	10.76
	Cruise	10.41	9.06	10.84
NB	Manual	17.46	15.20	17.28
	Cruise	18.38	15.67	17.71

estimates also demonstrate that the CCC driving is better than manual driving with regard to fuel economy (2.3 and 1.8 percent improvement, respectively).

The field data showed that the fuel economy of driving along the northbound test section of Interstate 81 was 73.8 percent greater than driving in the southbound direction. The VT-CPFM-1 and -2 model estimates also resulted in consistent outcomes given that the fuel economy values for driving along the northbound direction were estimated to be 71.1 and 61.9 percent greater, respectively, as illustrated in Figure 4. Consequently, the models appear to produce realistic and consistent conclusions as would be derived from field measurements.

4.3. Calibration of Model Parameters using Instantaneous Field Measurements

Since the VT-CPFMs, which are calibrated using the EPA ratings (referred to as EPA models hereafter), tended to overestimate fuel consumption levels, the calibration of the models was also conducted using the second-by-second OBD-gathered data (referred to as Field models hereafter) in order to ascertain the reason for these differences. Thus, the VT-CPFM parameters were calibrated using the instantaneous field measurements, as shown in Figure 5. Specifically, the field-measured fuel consumption rates were plotted versus the vehicle power estimates. A second-order polynomial was then fitted to the data. As seen in the figure, the EPA models for the Saab 95, the Mercedes R350, and the Chevy Malibu appear to be inconsistent with the field measurements while the Field models fit well to the measurements. These inconsistencies could be attributed to errors in estimating the instantaneous fuel consumption measurements assuming the fuel-to-air ratio is stoichiometric. Given that the errors appear at the high engine loads when the engine is running rich.

The differences in the fuel estimation are demonstrated in Figure 6 which features scatter plots and fuel consumption rates across the distance traveled. The scatter plots show the fuel consumption rates estimated by each of the EPA and Field models for the Mercedes R350 across the fuel consumption measurements. As can be seen in the figure, the Field model shows a significant improvement in the fuel estimation when compared to the EPA model. The subplots (c) and (d) also demonstrate that the fuel consumption estimated using the Field model is consistent with the field measurements.

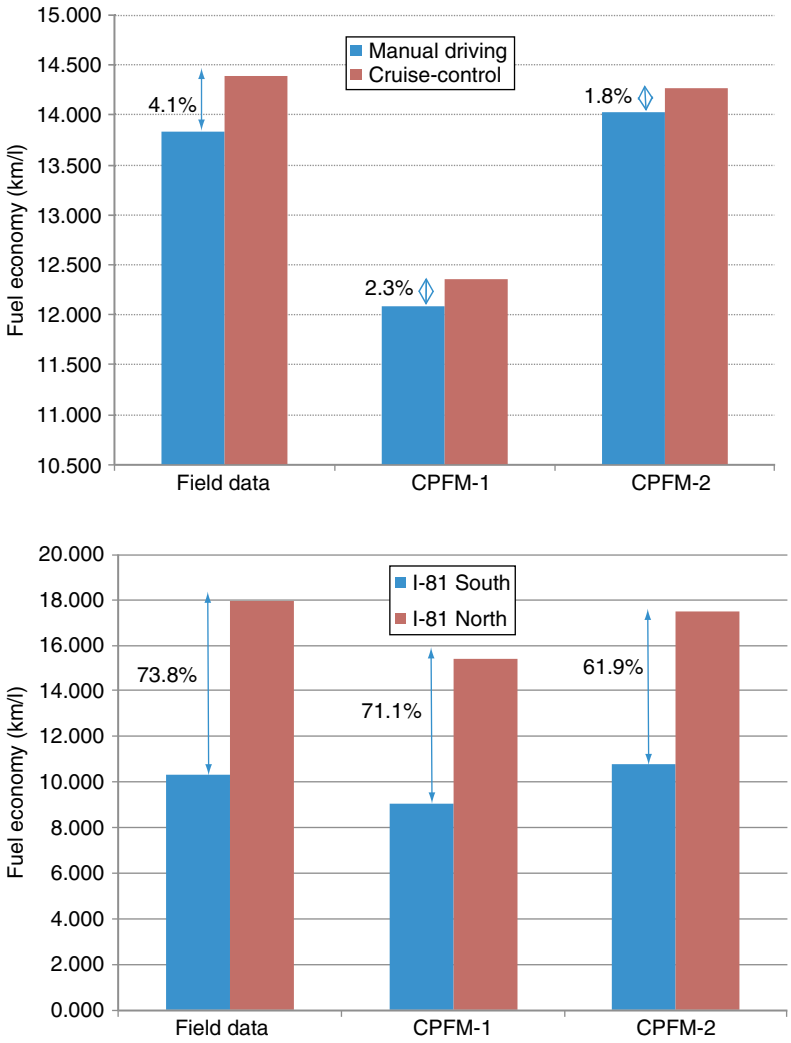

Figure 4. Comparison of field data with the VT-CPFM estimates

Given that the Field models fit the field measurements adequately, the city and highway fuel economy ratings were re-estimated by running the vehicle on the EPA drive cycles. The results demonstrate significant differences in the fuel economy ratings for some cases, as demonstrated in Table 5. For example, the highway fuel economy of the Mercedes R350 is rated at 21.0 MPG by the EPA, but is estimated at 29.6 MPG by

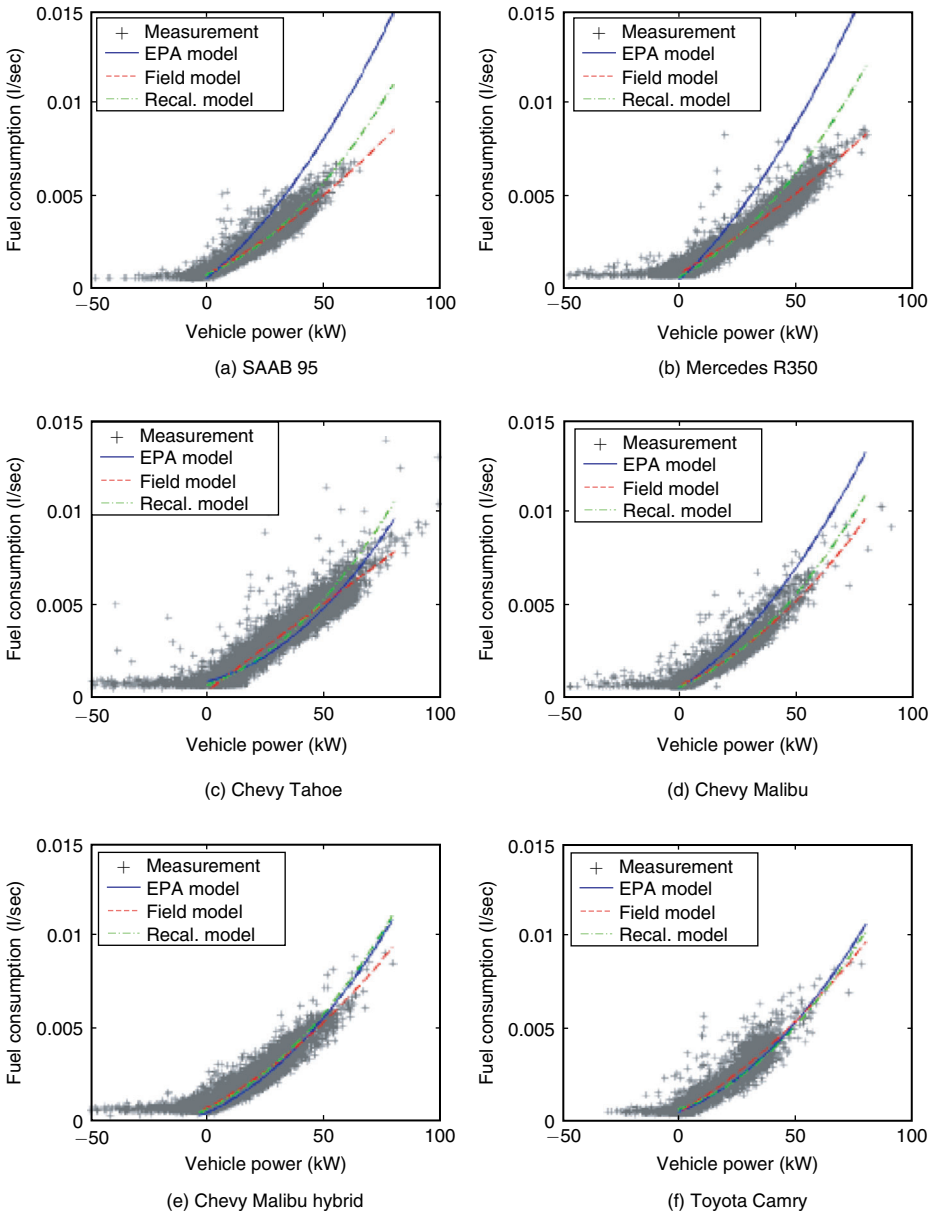

Figure 5. EPA, field, and recalibrated models

running the Field model on the EPA drive cycles. These results reveal that for some of the vehicles the EPA fuel economy ratings EPA are not consistent with what was observed in the field. These differences can either be attributed to errors in the

computation of the fuel rates based on the fuel-to-air ratio stoichiometric assumption, or could be attributed to errors in the EPA ratings, or errors in both. Regardless of the source of error, the objective of the study was to determine if the use of consistent EPA ratings with field measurements would result in good model predictions using the

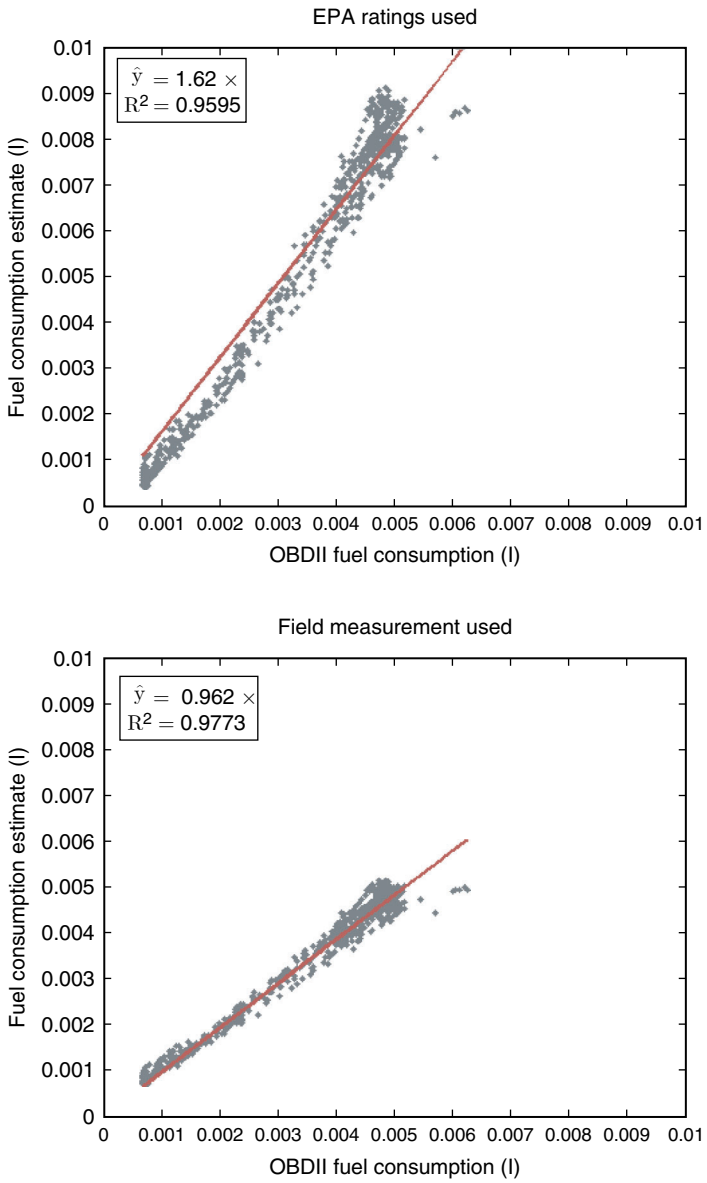

Figure 6. (*Continued*)

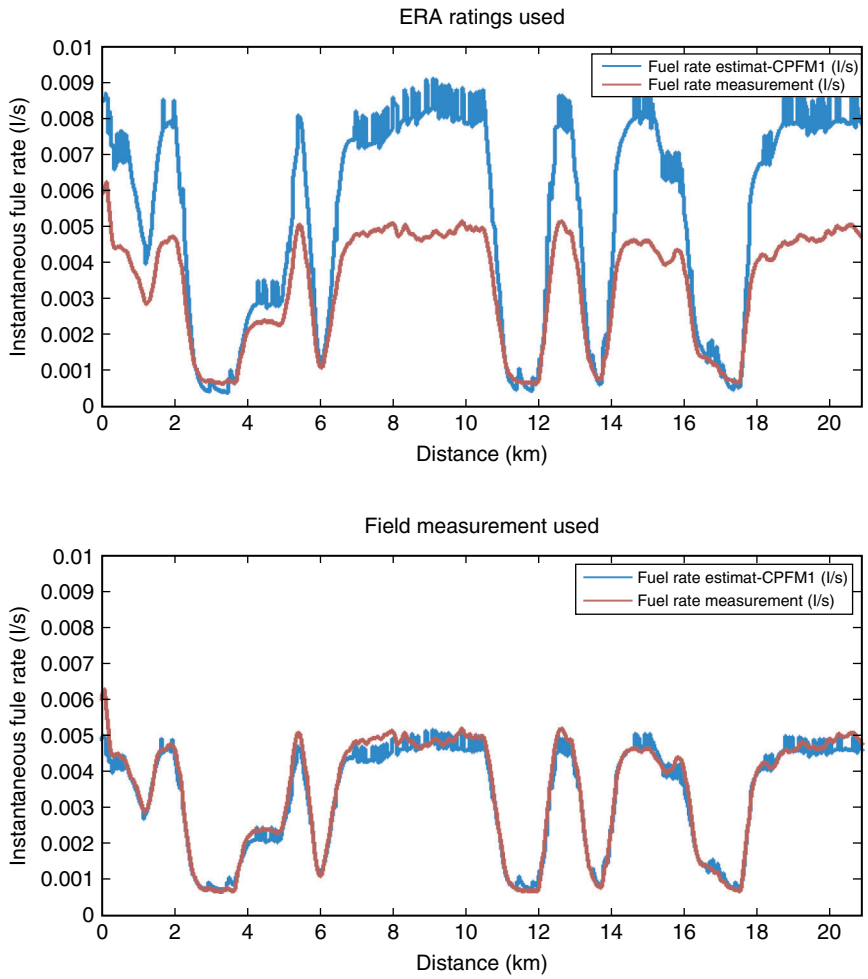

Figure 6. Comparison of fuel consumption estimates on a test run (Mercedes R350)

proposed calibration procedure. Consequently, in order to resolve this inconsistency the OBD fuel estimates were assumed to be correct and the EPA ratings were adjusted to match the field measurements.

In order to ascertain that the VT-CPFM framework is valid, the VT-CPFMs (referred to as Recalibrated models hereafter) were calibrated using the fuel economy ratings estimated based on the field measurements using Equations (4) through (7) then compared to the instantaneous field measurements. Once both sets of the models were consistent with each other with regard to the fuel consumption estimation, it was concluded that the structure of the VT-CPFM is valid and that the calibration procedure is also valid. As can be seen in Figure 5, the Recalibrated models fit the field

Table 5. Comparison of fuel economy ratings

	Fuel economy rated by EPA (MPG)		Fuel economy estimated by field model (MPG)		Relative difference	
Vehicle	City	Highway	City	Highway	City	Highway
Saab 95	21.0	30.0	23.3	38.9	11%	30%
Mercedes R350	16.0	21.0	18.7	29.6	17%	41%
Chevy Tahoe	17.3	27.7	23.7	28.1	37%	1%
Chevy Malibu	24.0	34.0	26.1	42.7	9%	26%
Hybrid Chevy Malibu	30.7	45.1	24.6	39.7	−20%	−12%
Toyota Camry	28.0	46.6	28.5	44.2	2%	−5%

Table 6. Summary of average slopes and R^2 values

	EPA model		Field model		Recalibrated model	
Vehicle	Slope	R^2	Slope	R^2	Slope	R^2
Saab 95	1.41	0.95	0.97	0.97	0.97	0.97
Mercedes R350	1.60	0.95	0.98	0.98	1.10	0.96
Chevy Tahoe	1.07	0.95	1.05	0.96	1.12	0.96
Chevy Malibu	1.29	0.96	1.00	0.97	0.99	0.97
Hybrid Chevy Malibu	0.95	0.96	1.00	0.97	1.00	0.97
Toyota Camry	0.97	0.90	1.02	0.90	0.93	0.84

measurements well, as do the Field models. Additionally, the slopes and R^2 values of the regression lines are fitted to the scatter plots of the fuel estimates computed by the Recalibrated models and the field measurements are as close to 1 as those of the Field models. The average slopes and R^2 values are summarized in Table 6 by test vehicle and model. As seen in Table 6, the Recalibrated models show a significant improvement in the fuel consumption estimation when compared to the EPA models. In other words, it can be concluded that the structure of the VT-CPFM provides a practical, valid method to estimate fuel consumption rates. In addition the source of error for some of the vehicles appears to arise from inconsistencies in EPA fuel economy ratings and those estimated using the field measurements.

5. SUMMARY FINDINGS AND CONCLUSIONS

The study validated the VT-CPFMs by comparing field-measured fuel consumption rates with model estimates. From the comparison results, the VT-CPFMs calibrated using the EPA city and highway fuel economy ratings are proven to generally provide reliable fuel consumption estimates. More importantly, both estimates and measurements have the same behavioral changes depending on engine load conditions. The study shows that the values of the coefficient of determination are close to 1.0, demonstrating the validity of the VT-CPFM. The proposed model can be integrated

within a traffic simulation framework to quantify the energy and environmental impacts of traffic operational projects. Furthermore, the proposed models can be used to develop predictive ECC systems and can be easily calibrated using publically available data.

REFERENCES

[1] H. A. Rakha, K. Ahn, K. Moran, B. Saerens, and E. V. d. Bulck, "Virginia Tech Comprehensive Power-Based Fuel Consumption Model: Model development and testing," *Transportation Research Part D: Transportation and Environment*, vol. Volume 16, pp. 492–503, 2011.

[2] B. Saerens, M. Diehl, and E. Van den Bulck, "Automotive Model Predicitive Control: Models, Methods and Applications," in *Lecture Notes in Control and Information Sciences*. vol. 402, ed Berlin/ Heidelberg: Springer, 2010, pp. 119–138.

[3] Drew Technologies Inc., "DashDAQ Series II - Instruction Manual," ed, 2010.

[4] B. van Arem, C. J. G. van Driel, and R. Visser, "The impact of cooperative adaptive cruise control on traffic-flow characteristics," *IEEE Transactions on Intelligent Transportation Systems*, vol. 7, pp. 429–436, Dec 2006.

[5] S. G. Kim, M. Tomizuka, and K. H. Cheng, "Smooth motion control of the adaptive cruise control system by a virtual lead vehicle," *International Journal of Automotive Technology*, vol. 13, pp. 77–85, Jan 2012.

[6] H. Rakha, I. Lucic, S. H. Demarchi, J. R. Setti, and M. Van Aerde, "Vehicle dynamics model for predicting maximum truck acceleration levels," *Journal of Transportation Engineering*, vol. 127, pp. 418–425, 2001.